

EFFICACY OF TYROSINE KINASE INHIBITORS IN THE MUTANTS OF THE EPIDERMAL GROWTH FACTOR RECEPTOR: A MULTISCALE MOLECULAR/ SYSTEMS MODEL FOR PHOSPHORYLATION AND INHIBITION

Jeremy E. Purvis¹, Yingting Liu², Vibitha Ilango³, and Ravi Radhakrishnan^{2*}

¹ Center for Bioinformatics, University of Pennsylvania,

² Department of Bioengineering, University of Pennsylvania,

³ Department of Electrical and Systems Engineering, University of Pennsylvania,
240 Skirkanich Hall, 210 S. 33 St., Philadelphia, Pennsylvania 19104

Abstract

Recent biochemical and epidemiological studies have shown that signaling through the epidermal growth factor receptor (EGFR) can be sensitive to various tyrosine kinase inhibitors (TKIs) depending on the receptor's expression level and whether or not the tyrosine kinase domain harbors somatic mutations. The rationale behind the varied response is still unclear, i.e., why certain cell-lines are hyper-sensitive to TKI treatment or how these inhibitors affect cell-wide signaling patterns, in particular, the attenuation of the oncogenic growth signals. In this work we provide a multiscale description of the interactions of wildtype and mutated EGFR systems with TKIs through a molecular/systems-level signal transduction model for quantifying and predicting the inhibitory effects on receptor phosphorylation and downstream signaling response. Our results suggest that the increased drug sensitivity observed for a commonly mutated form of EGFR, L834R, can be attributed to its altered kinetic behavior during receptor phosphorylation. Based upon our results, we conclude that the remarkable efficacy of the inhibitor erlotinib in the L834R mutant cell line can be attributed to relative gain in efficiency over the wildtype (WT) in inhibiting the Akt response.

Keywords

Epidermal Growth Factor Receptor, L834R, Multiscale Model, Tyrosine Kinase Inhibitor, Receptor-mediated Signaling

*To whom all correspondence should be addressed; email: rradhak@seas.upenn.edu

INTRODUCTION

Members of the Erb family of receptors — the epidermal growth factor receptor (EGFR/ErbB1/HER1), ErbB2, ErbB3, and ErbB4 — activate a multi-layered network mediating crucial pathways leading to cell proliferation and differentiation (CitriYarden 2006), in response to activation of the receptors by the epidermal growth factor (EGF), transforming growth factor- α , and several other related peptide growth factors (CitriYarden 2006). Over-expressions of EGFR and ErbB2 are correlated with a variety of clinical cancers. Hence, small molecule tyrosine kinase inhibitors (TKIs) for EGFR/TK and ErbB2 RTK, e.g., gefitinib and erlotinib, which are ATP analogues, are of significant interest as cancer therapeutic drugs. While the RTK inhibition approach has shown promise in some clinical trials, results have been quite mixed. In particular, the occurrence of somatic mutations in the EGFR kinase domain (L834R, L837Q, G685S, del L723-P729 ins S) as seen in non-small-cell lung cancers (Sordella et al. 2004; Carey et al. 2006) render the cell lines harboring such mutations more sensitive to TKI treatment; these clinical mutations in an alternative scheme are denoted by L858R, L861Q, G719S, del L747-P753 ins S. In vitro, these EGFR mutants demonstrated enhanced tyrosine kinase activity in comparison to wildtype EGFR and increased sensitivity to inhibition (Sordella et al. 2004).

Previously, we employed a hierarchical multiscale computational strategy to study the dimer-mediated receptor activation characteristics of the Erb family receptors, through which we were able to transcribe the effects of molecular alterations in the receptor (e.g., mutant forms of the receptor) to differing kinetic behavior and downstream signaling response (Liu et al. 2007). Here, we extend this approach to study the effects of EGFR inhibition through TKIs. By employing molecular docking in combination with network modeling, we are able to quantify changes in the EC_{50} of receptor phosphorylation (i.e. 50% inhibition in the cellular context), and EC_{50} for the inhibition of downstream markers (ERK and Akt) upon treatment with the TKI erlotinib, in cell-lines carrying both wildtype (WT) and mutant forms of the receptor. Based upon our results, we conclude that the remarkable efficacy of the inhibitor erlotinib in the L834R mutant cell line can be attributed to relative gain in efficiency over the WT in inhibiting the Akt response.

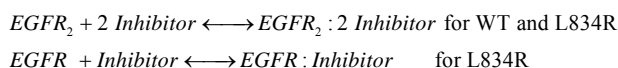
METHODS

Signal Transduction Model

Models for the WT and L834R systems each comprised 74 species, 140 parameters, and 77 reactions and are described in detail in our recent work (Liu et al. 2007). The model parameters are derived from previously

published models (Kholodenko 2006), and de novo molecular level calculations in our lab (Liu et al. 2007). A complete model description is provided as an appendix in the Supplementary Material and an SBML file of the model is available upon request. One important difference between the WT and L834R mutant network is that the WT RTK initiates phosphorylation of C-terminal tail substrate tyrosines only as a dimer, whereas the mutant, owing to constitutive activation, can initiate phosphorylation as a monomer as well as a dimer (Zhang et al. 2006). Our molecularly resolved signal transduction network incorporates differential signaling through Y1068 and Y1173 phosphorylation sites of the EGFR/TK (see differential signaling through Y1068 and Y1173, below).

To model competitive inhibition by an ATP analog, we employed the following reactions in our model.



Consistent with our computational studies (our molecular docking studies described below revealed that the ATP binding affinity of the RTK in the inactive state is 100-fold lower than that in the active state), the above reactions are implemented as several analogous reactions, such that an inhibitor molecule may bind to the activated receptor kinase when the substrate tyrosines are unphosphorylated, or already phosphorylated at either Y1068 or Y1173. To model the kinetic behavior in the presence of the TKI erlotinib, we used appropriate values for the inhibition constant (K_I) of erlotinib, binding constant for ATP, and constants for describing the phosphorylation kinetics of Y1068 and Y1173 peptides for WT and mutant (L834R) receptors. These parameters are obtained from our molecular-level simulations (see section: Molecular Docking, below), and from experiments. The parameters are summarized in Table 1.

Table 1. Parametric differences between WT and mutant EGFR systems

<i>Parameter</i>	<i>WT</i>	<i>L834R</i>	<i>Ref.</i>
K_M^{ATP}	5.0 μM	10.9 μM	1
$K_I^{\text{erlotinib}}$	17.5 nM	6.25 nM	1
K_M^{Y1068}	265 μM	13.3 μM^*	2, 3
K_M^{Y1173}	236 μM	944 μM^*	2, 3
$k_{\text{cat}}^{\text{Y1068}}$	0.29 s^{-1}	0.14 s^{-1*}	2, 3
$k_{\text{cat}}^{\text{Y1173}}$	0.25 s^{-1}	0.010 s^{-1*}	2, 3

1=(Carey et al. 2006); 2=(Fan et al. 2004); 3=(Liu et al. 2007); *Calculated from molecular simulations

Systems-level Model Calibration using Genetic Algorithm: Model parameters were refined by calibrating simulation output with data from published cell-base assays and time-resolved mass spectrometry (Zhang et al. 2005). A genetic algorithm (GA) was used to identify

parameter-sets that produced the closest fit to time course measurements, using a linear least squares distance measure between computed and measured time course data points as the objective function.

Initial estimates (default) of parameters were taken from published studies, or computed by molecular docking and stochastic simulations as described previously (Liu et al. 2007). In the GA, each parameter value was sampled from a log-normal distribution (μ = default value, σ = 1 log unit) to allow the parameters (rate constants or initial conditions, except those for [EGFR], [EGF], and [TKI]) to range continuously over several orders of magnitude, but with strong central tendency for the default value. The GA was implemented with a constant-sized population of 100 parameter sets (individuals), mutation rate μ = 0.15, and crossover rate ρ = 0.15, for 1000 generations. Fitness scores for all individuals were evaluated at each generation by computing the objective function.

Model Sensitivity using Principal Component Analysis: In order to obtain a quantitative measure of the sensitivity and robustness of the signaling-network to rate-constants and initial concentrations, we employed a Monte Carlo protocol to perturb the default parameter sets. This was done by generating a random vector of elements ζ_i from a normal distribution with mean zero and variance (σ) 0.3, 1.0, and 3.0, then perturbing the default parameters P_i as $P_i \times \exp(\zeta_i)$. Network simulations were repeated 2000 times with new (perturbed) parameter-sets and the sets yielding top 500 values for ERK and Akt activation were stored. A principal component analysis in parameter-space (over the 500 stored sets) was carried out in order to determine the combinations of parameters (i.e., the constitution of the principal eigenvectors), whose perturbation are likely to render the signaling hyper-active to ERK and Akt phosphorylation, that is, phosphorylation of ERK/Akt in the perturbed system is greater than in the unperturbed system. These calculations were performed in two contexts: (1) by choosing the set of rate-constants as the parameters P_i , and (2) by choosing the set of initial concentrations as the parameters P_i .

Differential Signaling through Y1068 and Y1173: Our molecular resolution to the systems model stems is enabled by two features in our research design. (1) By the *de novo* estimation of key binding and rate-constants associated with the receptor through molecular simulations (see section below), we are able to quantify the molecular contributions to signaling and hence differentiate signaling in WT and mutant cells. (2) Our systems model introduces the concept of differential signaling, where phosphorylation at the Y1068 and Y1173 sites transduce signals through different pathways. This differential effect was initially incorporated based on experimental evidence (Sordella et al. 2004) by assuming perfect (or 100/0) specificities for the interactions of the Y-phosphorylated docking sites: i.e., the phosphorylated Y1068 binds only to PI3K and Grb2 and not PLC γ and Shc, and phosphorylated Y1173 binds only to PLC γ and Shc and not to PI3K and Grb2. The other end of the spectrum is to

assume no (50/50) specificity, i.e., the two sites 1068 and 1173, when phosphorylated, serve as docking sites to all four substrates in our model, namely PI3K, Grb2, PLC γ and Shc. This would reduce to a single-site model, where the docking sites are not distinguished. A realistic model for incorporating this differential effect lies between these two extremes. The degree to which the docking interactions of the phosphotyrosines are specific can be determined by molecular docking calculations similar to those described in the section below (these calculations are on going in our laboratory). However, in order to gauge the sensitivity of the downstream response (ERK vs. Akt activation) on the degree of specificities, we performed network simulations with varying degrees of specificities ranging from 100/0 to 50/50.

Molecular Docking

We employ AutoDock, an automated docking tool designed to predict how small molecules, such as substrates or drug candidates, bind to a receptor of known 3-dimensional structure (Morris et al. 1998). The binding free energy is calculated based on the intermolecular energy between protein and ligands and torsional and solvation free energy of the ligands (Morris et al. 1998). We perform a global conformational search using a multiple conformation docking strategy (the multiple conformations generated through fully atomistic explicit water molecular dynamics simulations), in which the protein flexibility is taken into account implicitly.

By employing this method, we computed the K_I for WT and L834R mutant RTK binding to erlotinib, and to two peptide sequences consisting of Y1068 and Y1173. This data, reported in Table 1, is used to parameterize the reactions involving inhibitor binding and substrate phosphorylation in the systems model.

We have also employed the Bell (Bell 1978) model in obtaining the sensitivity of the bound peptide sequence on peptide phosphorylation rates. Namely, by assuming a harmonic energy profile along the reaction coordinate ξ with a force constant K_ξ , the work done in reducing this distance is given by $1/2K_\xi\xi^2$ and the corresponding reduction in the phosphorylation (turn-over) rate is taken as $\exp(-K_\xi\xi^2/2k_B T)$. The value of K_ξ is obtained by recording the standard deviation σ_ξ in the positional fluctuations of ξ in our molecular dynamics simulations, i.e., $K_\xi = k_B T / \sigma_\xi^2$. The values of the peptide-dependent phosphorylation rate, k_{cat} , thus obtained for WT and mutant receptors are also reported in Table 1.

RESULTS AND DISCUSSION

Differential phosphorylation: We first assessed the differential phosphorylation patterns of WT EGFR and L834R mutant systems, with normal receptor copy number (initial [EGFR] = 100 nM or 30,000 receptors per cell), with 8 nM (50 ng/ml) EGF or without EGF stimulation (Fig. 1). As expected from the altered K_M and k_{cat} values, L834R has a stronger preference for Y1068

phosphorylation compared to the WT receptor, while our results predict the opposite trend for Y1173 phosphorylation.

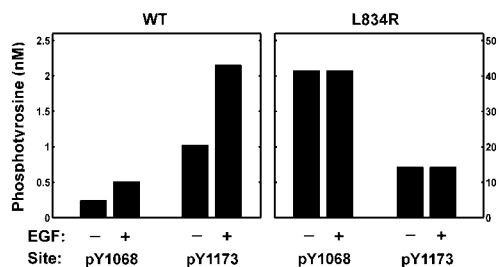


Figure 1. Differential signaling for WT and L834R. Total phosphotyrosine (pY1068 or pY1173) was calculated after 60 s, with (8 nM) and without ligand (EGF).

Differential Signaling: To examine the effects of our branched signaling through pY1068 and pY1173 on the downstream response, we explored a series of cases in which differential signaling was fully implemented i.e. 100/0 (see methods section), partially active (75/25), or completely absent (50/50). In the latter case, docking peptides (e.g., PLC γ , PI3K, Gab1) could bind indiscriminately to either phosphorylated tyrosine sites. Simulations were performed for 15 min (900 s) with 8 nM EGF present. The resulting total pERK and pAkt response are reported in Fig. 2.

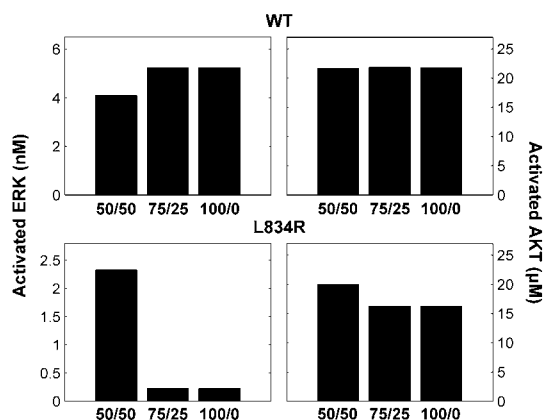


Figure 2. Effect of branched signaling on downstream response: no/partial/full signal branching (50/50)/(75/25)/(100/0).

For both systems, implementing either a partially or completely specific branching quantitatively yields the same downstream response, regardless of the degree of differential signaling. This observation validates our hypothesis that the differences in the downstream signaling between the WT and mutant receptors stem from changes in the efficiency of C-terminal tail phosphorylation (i.e., k_{cat}/K_M values for the substrate

tyrosines) rather than the specificities of the docking proteins to phosphotyrosines. One notable feature is the 10-fold lower pERK levels in the mutant in the presence of a differential branched signaling, suggesting that specificity of the Y1173 peptide induces a sensitivity in the ERK activation, but the degree of specificity (when present) is unimportant.

Robustness of Signaling: In a recent review, the ErbB signaling network is described as a bow-tie-configured (or hour-glass shaped), evolvable network, displaying modularity, redundancy, and control circuitry (CitriYarden 2006). This framework suggests that identifying the targets proteins for effective inhibition and the effects of the mutation landscape would require a systems level understanding of the signaling network. Based on the protocol outlined in the methods section, we perturbed the network using our Monte Carlo strategy and performed principal component analysis in the space of rate-constants as well as on initial concentrations. In both cases, the top three modes constituted 99% of the scatter in the parameter space. We then identified the components of the three principal eigenvectors (i.e., which particular combination parameters render the network hyper-sensitive according to our measure.

Table 2. Parameter variations constituting the top three principal components for network hyper-sensitivity.

Rate Constants	Initial Concentrations
k_f : Y1068	[Raf•Ras•GTP]
k_f : Y1173	[Pase3] phosphatase for pERK
K_M : ATP•RTK	[pMEK]
K_M : GAB•pEGFR	[PI3K inactive]
	[MEK•Raf active]
	[EGFR•Shc•Grb2•SOS•RasGTP]

k_f : turn-over for phosphorylation; •: bound complex;

There were several surprising features in our findings: (1) The components of the eigenvectors were non-zero only as singlets or pairs, suggesting that the perturbation of only one or at most a combination to two parameters were driving the network hyper-sensitive; (2) The identified components (see Table 2), were insensitive to the degree of perturbation (i.e., the same components resulted irrespective of the extent of perturbation, σ of 0.3, 1.0, and 3.0); (3) The resulting components in Table 3 clearly reflect the bow-tie-configuration of the network, namely, the system is susceptible to perturbation only at the top (and bottom, these are our measures for hyper-sensitivity), with the middle (or core) layers robust to perturbations; (4) The top principal components identified almost exclusively comprised of ATP binding and C-terminal tyrosine phosphorylation, thereby justifying why the inhibition of receptor phosphorylation is likely to be

an optimal target, and suggesting why mutations changing the (differential) phosphorylation kinetics can profoundly impact the downstream response.

EC₅₀ for Inhibition of EGFR in the cell. Next, we examined the sensitivity of WT and mutant systems to inhibition in the cellular context by calculating receptor phosphorylation over a range of erlotinib concentrations. Simulations were performed for both ‘normal’ ([EGFR] = 100 nM) and ‘over-expressed’ ([EGFR] = 1000 nM) systems. All simulations were performed with (50 ng/ml or 8 nM) or without ligand (EGF) stimulation.

The EC₅₀ (inhibitor concentration at which 50% of the activity is suppressed in the cellular context; this is different from IC₅₀ because the non-linear and temporal effects due to signal-transduction is accounted for) for L834R was 50-fold lower (see Fig. 3: a,b) than that of the WT (100 nM vs. 5000 nM) in the presence as well as absence of ligand. There were also no prominent differences between the inhibition at 1068 and 1173 sites. In over-expressed systems, there was no significant difference in EC₅₀ among the four groups (Fig. 3: c,d). All had an EC₅₀ near 1000 nM.

Inhibition of Downstream Activation (EC₅₀): We then examined the sensitivity of downstream signaling molecules ERK and Akt to inhibition for a range of erlotinib concentrations (see Figure 4: a-d).

In normal expression systems (Fig. 4: a,b), there was a nearly 7-fold increase in the efficiency of pERK inhibition for L834R (EC₅₀ = 100 nM) compared to WT (EC₅₀ = 700 nM) with and without ligand present. With respect to Akt activation, there was a 4-fold decrease in EC₅₀ for L834R compared to WT (300 nM vs. 1200 nM) with and without ligand present. For the case of over-expressed receptors (Fig. 4:c,d), inhibition of pERK is 4-fold more efficient for L834R compared to WT, while pAkt inhibition is almost 10-fold more efficient for the L834R mutant, although significantly more erlotinib is required to achieve inhibition (EC₅₀=40 μM). This result is consistent with the dramatically elevated Akt levels expected in systems that bear both the L834R mutation and a higher receptor count.

CONCLUSION

We have presented a framework to interpret the effect of tyrosine kinase inhibitors on the system-wide response. Through multiscale modeling, we have also shown how this framework can be utilized to predict the efficacy of the inhibition in cell-lines, especially those harboring mutations in the receptor. We find that the mutant cell line is more susceptible to inhibition by TKIs both at the level of curbing the receptor phosphorylation as well as that of downstream (ERK and Akt) activation. Considering that the absolute pAkt levels are 5-fold higher than those for pERK in the WT and 100-fold higher in the mutant (Fig. 2), the remarkable effect of the drug in non-small-cell lung cancer cell lines carrying the mutation can be attributed to the gain in efficacy with respect to Akt inhibition.

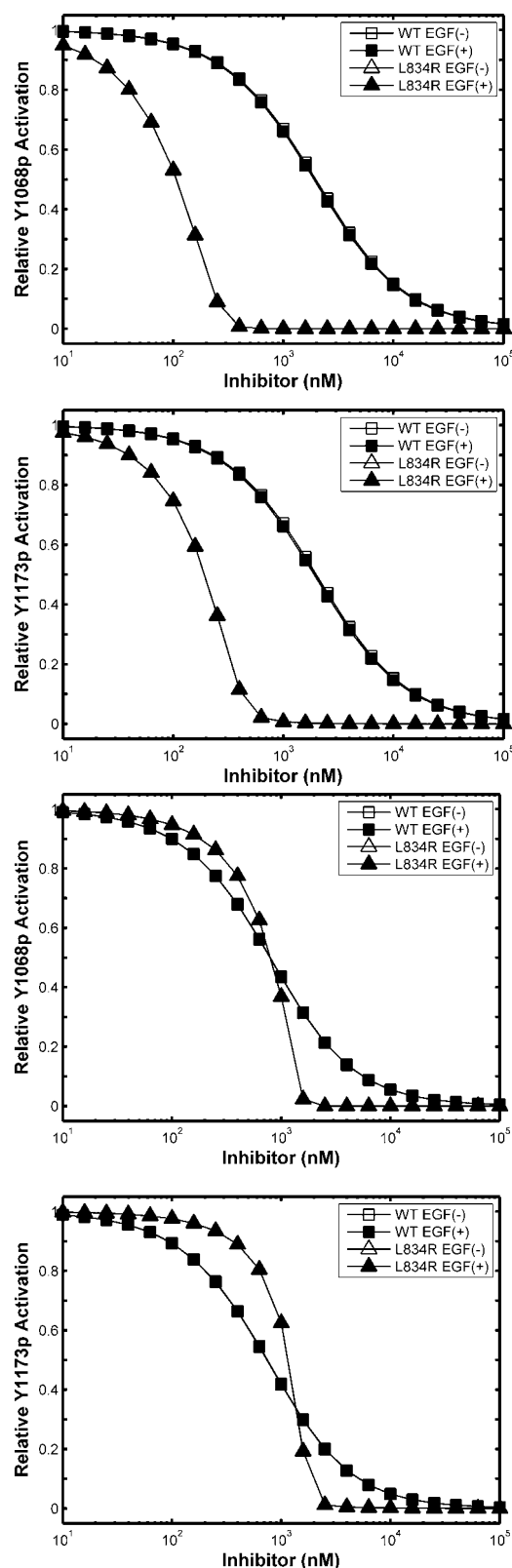


Figure 3. Relative inhibition of receptor phosphorylation: Tyr phosphorylation levels relative to that without inhibitor are plotted.

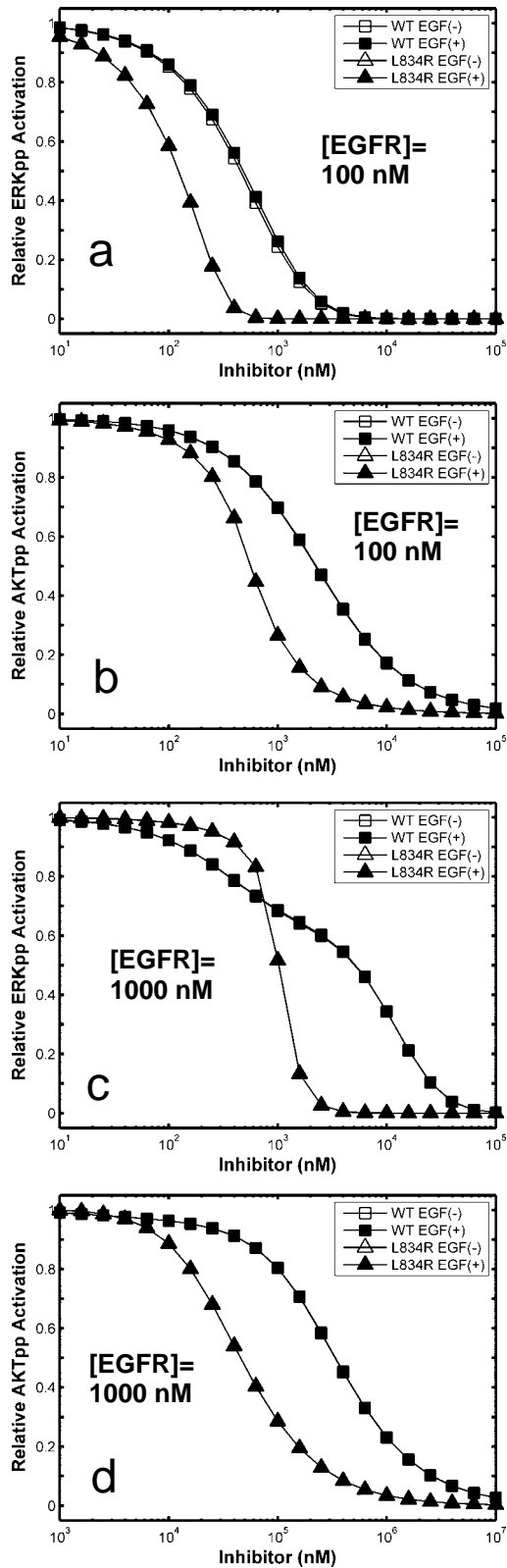


Figure 4. Inhibition of ERK and Akt activation in systems with normal receptor expression. Responses plotted relative to that without inhibition under the same conditions.

The multiscale computational framework described here is ideal for assessing mutation landscape on signal transduction. We believe that our model driven approach will in the long-term significantly impact the optimization of future small molecule therapeutic inhibition strategies.

ACKNOWLEDGMENTS

We thank Mark A Lemmon and Sung-hee Choi for numerous discussions. Funding for this work was in part from the Whitaker Foundation and the Greater Philadelphia Bioinformatics Alliance. Computational resources were provided in part by the NPACI Grants DAC1103423 and MCB060006. Supplementary material is available online.

REFERENCES

- Bell, G. I. (1978). Models for the specific adhesion of cells to cells. *Science*. 200. 618.
- Carey, K. D., et al. (2006). Kinetic analysis of epidermal growth factor receptor somatic mutant proteins shows increased sensitivity to the epidermal growth factor receptor tyrosine kinase inhibitor, erlotinib. *Cancer Research*. 66. 8163-8171.
- Citri, A. and Y. Yarden (2006). EGF-ERBB signalling: towards the systems level. *Nat Rev Mol Cell Biol*. 7. 505-16.
- Fan, Y. X., et al. (2004). Ligand regulates epidermal growth factor receptor kinase specificity - Activation increases preference for GAB1 and SHC versus autophosphorylation sites. *Journal of Biological Chemistry*. 279. 38143-38150.
- Kholodenko, B. N. (2006). Cell-signalling dynamics in time and space. *Nat Rev Mol Cell Biol*. 7. 165-76.
- Liu, Y., et al. (2007). A Multiscale Computational Approach to Dissect Early Events in the Erb Family Receptor Mediated Activation, Differential Signaling, and Relevance to Oncogenic Transformations. *Annals of Biomedical Engineering*.
- Morris, G. M., et al. (1998). Automated Docking Using a Lamarckian Genetic Algorithm and an Empirical Binding Free Energy Function. *J. Comput. Chem.*, 19. 1639-1662.
- Sordella, R., et al. (2004). Gefitinib-sensitizing EGFR mutations in lung cancer activate anti-apoptotic pathways. *Science*. 305. 1163-7.
- Zhang, X., et al. (2006). An allosteric mechanism for activation of the kinase domain of epidermal growth factor receptor. *Cell*. 125. 1137-49.
- Zhang, Y., et al. (2005). Time-resolved mass spectrometry of tyrosine phosphorylation sites in the epidermal growth factor receptor signaling network reveals dynamic modules. *Molecular & Cellular Proteomics*. 4. 1240-1250.

Supporting Material for “Efficacy of Tyrosine Kinase Inhibitors in the Mutants of the Epidermal Growth Factor Receptor: A Multiscale Molecular/ Systems Model for Phosphorylation and Inhibition”

Jeremy Purvis, Yingting Liu, Vibitha Ilango, and Ravi Radhakrishnan

Systems Models for Wild-type and L834R Systems

Deterministic, Ordinary Differential Equations-based systems models are constructed as described previously [1]. EGF stimulation in a cell results in the simultaneous activation of multiple pathways that are functionally interlinked [2-4]. The major pathways we include in our model are: (1) *EGF-ERK route*. A major downstream signaling cascade triggered by the activation of EGFR [5] is the Ras-Raf-MAP-kinase pathway [6-12]. Activation of Ras initiates a multistep phosphorylation cascade that leads to the activation of MAPKs, ERK1, and ERK2. ERK1 and ERK2 regulate transcription of molecules that are linked to cell proliferation, survival, and transformation. (2) *Phosphoinositol Metabolism and Signaling*. Activation of EGFR TK leads to rapid stimulation of phosphoinositol metabolism and generation of multiple second messengers [13-17]. PLC γ is rapidly recruited by an activated RTK through the binding of its SH2 domains to pTyr sites in the receptor molecules. Upon activation PLC γ hydrolyzes its substrate PtdIns(4,5)P₂ to form two second messengers, diacylglycerol and Ins(1,4,5)P₃. By binding to specific intracellular receptors, Ins(1,4,5)P₃ stimulates the release of Ca²⁺ from intracellular stores. Ca²⁺ then binds to calmodulin, which in turn activates a family of Ca²⁺/calmodulin-dependent protein kinases. In addition, both diacylglycerol and Ca²⁺ activate members of the PKC family of protein kinases. The second messengers generated by PtdIns(4,5)P₂ hydrolysis stimulate a variety of intracellular responses in addition to phosphorylation and activation of transcriptional factors. (3) *PI3K-Akt pathway*. Another important target in EGFR signaling is phosphatidylinositol 3-kinase (PI3K) and the downstream protein-serine/threonine kinase Akt. Prior studies have established that some growth hormone-stimulated membrane tyrosine kinase receptors interact with Shc adapter protein and phosphatidylinositol 3'-kinase (PI3K), and consequently PI3K-activated Akt inhibits Raf-1 and the following ERK activity [18-21]. Akt transduces signals that trigger a cascade of responses from cell growth and proliferation to survival and motility [5, 22-24]. The pathways we do not include in our model are: (4) *Nuclear Translocation of STATs*. EGF stimulation leads to rapid tyrosine phosphorylation and migration of STATs to the nucleus and transcription of target DNA genes [3]. (5) Also, there is evidence of a c-Src mediated functional link between EGFR TK activation and STAT5 [25-28]. (6) EGFR expression is negatively regulated by the process of clathrin mediated endocytosis [29] through cbl-CIN85-endophilin interactions [30, 31]. (7 and 8) External signals can also be transduced by molecular cross-talk in which other receptors (e.g., GPCR, integrins) signal using the EGFR network [32-38].

In the kinetic model employed here, signaling through the EGFR is modeled by combining three published models and augmented by our own set of reactions and calculations. Phosphorylation and docking reactions are modeled according to Ref. [8]; the MAP kinase pathway reactions are modeled after Ref. [12]; Akt and PI3K activation are incorporated into the model as described in Ref. [19]. The similar parameterization and topology in these models allows us to construct a consistent, stable, and comprehensive system with results in good agreement with published experimental data [39]. Altogether, our model comprises of 74 reactions and 67 species. 17 of these reactions are novel to this work and represent enhanced molecular resolution and detail in EGFR activation, phosphorylation, and docking reactions.

System Models for wild-type and mutant (L834R) systems are assembled using the Systems Biology Markup Language (<http://sbml.org>), facilitated by the SBML short-hand language (<http://www.staff.ncl.ac.uk/d.j.wilkinson/software/sbml-sh/>), which was used to present the full model below (Table S1). In the model description which follows, SBML component names (e.g., reactions, species, parameters) are presented in italics for reference. Figure S1 shows a schematic of the early signaling events.

Ligand Binding and Dimerization (Fig. S1, 1,2). EGF binding to receptor (*LigandBinding*) is modeled as described by Kholodenko [8]. Dimerization of activated monomers (Fig. S1, 2; *Dimerization2*) is also modeled according to this scheme, although two additional dimerization reactions are added to represent spontaneous association of unactivated monomers (*Dimerization0*) and activated-unactivated dimer pairs (*Dimerization1*). For these two non-specific interactions, an off-rate of 1000 s⁻¹ is used ($k_{offDimer0}$, $k_{offDimer1}$), which is 10,000-fold faster than the specific interaction between activated monomers. Thus, this baseline dimerization is essentially diffusion controlled.

Dimer Binding ATP (Fig. S1, 3). In our molecularly resolved model, all forms of the dimer bind ATP at the same rate, although the Michaelis constant differs between wild-type and mutant systems (see Table 1 in main text). The reactions are *Dimer0BindingATP*, *Dimer1BindingATP*, and *Dimer2BindingATP*. Receptors which have already phosphorylated one of the two modeled tyrosine phosphorylation sites may also bind ATP. These reactions are *Dimer0Y1068pBindingATP*, *Dimer0Y1173pBindingATP*, *Dimer1Y1068pBindingATP*, *Dimer1Y1173pBindingATP*, *Dimer2Y1068pBindingATP*, and *Dimer2Y1173pBindingATP*. In the mutant system, the following reactions are added to reflect binding of ATP to the monomeric receptor (*EGFRBindingATP*, *EGFRaBindingATP*):



For each of the ATP binding reactions, we used the published value of $K_M = 2.4 \times 10^{-8} \text{ M}^{-1}$ [40] and added an extra term in the rate law to reflect competitive inhibition by the inhibitor TKI (*Inh*):

$$(2) \quad \frac{[DIMER] \cdot [ATP]}{K_{ATP} \cdot (1 + ([Inh] / K_{Inh}))}$$

The same reaction scheme is used to model inhibitor binding to the receptor (*EGFRBindingInh*, *EGFRaBindingInh*),



with competitive binding by ATP:

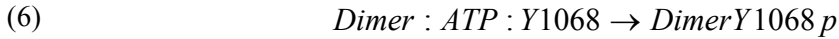
$$(4) \quad \frac{[DIMER] \cdot [Inh]}{K_{Inh} \cdot (1 + ([ATP] / K_{ATP}))}$$

Peptide Entering Catalytic Zone (Fig. S1, 4). Fast reactions representing intramolecular diffusion of the receptor's cytoplasmic tail (*Y1068nearsDimer0*, *Y1068nearsDimer0Y1068p_ATP*, *Y1068nearsDimer1*, *Y1068nearsDimer1Y1068p_ATP*, *Y1068nearsDimer2*, *Y1068nearsDimer2Y1068p_ATP*) are modeled as described below and in [1]. The following scheme is used for all forms of the receptor involving diffusion of tyrosine 1068 (Y1068):



The calculated on-rate for diffusion of Y1068 is 650800 s^{-1} and the off-rate was 38.5 s^{-1} . The same scheme is used for diffusion of Y1173 ($Y1173nearDimer0$, $Y1173nearDimer0Y1173p_ATP$, $Y1173nearDimer1$, $Y1173nearDimer1Y1173p_ATP$, $Y1173nearDimer2$, $Y1173nearDimer2Y1173p_ATP$). The on-rate for diffusion of Y1173 is 198400 s^{-1} and the off-rate is 192.4 s^{-1} . For the mutant system, an additional four reactions ($Y1068nearEGFR_ATP$, $Y1068nearEGFRa_ATP$, $Y1173nearEGFR_ATP$, $Y1173nearEGFRa_ATP$) are necessary to account for diffusion reactions for the activated monomer.

Catalysis of Phosphorylation (Fig. S1, 5,6). Irreversible phosphorylation reactions are constructed for each of the activated dimers ($PhosphorylationOfDimer0_ATP_Y1068$, $PhosphorylationOfDimer0Y1068p_ATP_Y1068$, $PhosphorylationOfDimer1_ATP_Y1068$, $PhosphorylationOfDimer1Y1068p_ATP_Y1068$, $PhosphorylationOfDimer2_ATP_Y1068$, $PhosphorylationOfDimer2Y1068p_ATP_Y1068$, $PhosphorylationOfDimer0_ATP_Y1173$, $PhosphorylationOfDimer0Y1173p_ATP_Y1173$, $PhosphorylationOfDimer1_ATP_Y1173$, $PhosphorylationOfDimer1Y1173p_ATP_Y1173$, $PhosphorylationOfDimer2_ATP_Y1173$, $PhosphorylationOfDimer2Y1173p_ATP_Y1173$) and mutant monomers ($PhosphorylationOfEGFR_ATP_Y1068$, $PhosphorylationOfEGFRa_ATP_Y1068$, $PhosphorylationOfEGFR_ATP_Y1173$, $PhosphorylationOfEGFRa_ATP_Y1173$) with peptides located in the catalytic zone (products of reactions described immediately above). Reactions followed the general scheme shown below for Y1068.



Turnover rates for the wild-type system are 0.29 s^{-1} for Y1068 and 0.25 s^{-1} for Y1173 as reported by Fan [41]. Turnover rates for the mutant are calculated from molecular simulations and are 0.14 s^{-1} for Y1068 and 0.010 s^{-1} for Y1173.

Dephosphorylation Reactions. Dephosphorylation reactions affecting both peptides ($DephosphorylationOfY1068p$ and $DephosphorylationOfY1173p$) are implemented as described by Kholodenko [8], using Michaelis constant $K_M = 50 \text{ nM}$ and $V_{MAX} = 450 \text{ nM s}^{-1}$. Note that, in order to prevent proliferation of model species, all phosphorylated receptor forms are grouped into two “pseudo-species” ($TotalY1068p$ and $TotalY1173p$) which are also included as SBML products in the phosphorylation reactions described above.

Intramolecular Diffusional and C-terminal Tail Tyrosine Auto/ Trans-Phosphorylation Auto- as well as trans-phosphorylation of specific tyrosine sites in the C-terminal tail of the receptor involves diffusion of the particular tyrosine residue in the C-terminal tail to the active site of the EGFRTK. Based on the crystal structure of Stamos [42] and the dimer interface identified by Kuriyan [43], we identify the unstructured region of the C-terminal tail as constituted by residue 960 onwards. The seven tyrosine residues present on each tail will then have a characteristic time of diffusion to the active site. We model the tail from residue 960 to the particular tyrosine residue of interest as a freely joined chain (FJC) consisting of Kuhn segments [44]; a persistence length of 3.04 \AA is used following the results of Zhou [45]. According to the FJC model, the spatial distribution of one end of the FJC with coordinates x,y,z (where the tyrosine residue is located) with the other end (residue 960) fixed at origin is described by a Gaussian distribution at thermal equilibrium:

$$P(x,y,z) = [3/(2\pi N_K b^2)]^{3/2} \exp[-3(x^2+y^2+z^2)/(2N_K b^2)],$$

where, $P(x,y,z)$ is the probability of finding the tyrosine residue at coordinates (x,y,z) , N_K is the number of Kuhn segments between the fixed end and the tyrosine residue, and b is the Kuhn length (twice the persistence length) of the protein ($\sim 6.08 \text{ \AA}$). The diffusion coefficient of the tyrosine residue is then calculated using reptation model [44]:

$$D = (k_B T)/(6 \pi N_K \mu a),$$

where, D is the diffusivity of the tail, k_B is the Boltzmann constant, T is the temperature (300 K), N is the number of residues between the fixed end and tyrosine residue, μ is the viscosity (8.9×10^{-4} Ns/m²), and a is the hydrodynamic radius of a single amino acid residue (1.9 Å).

Using transition state theory, the rate of tyrosine binding to the active-site was calculated as the product of the probability of the tyrosine residue to reach the active-site, i.e. $P(x^*, y^*, z^*)$, and the characteristic relaxation frequency of the tyrosine residue, i.e., D/a^2 ; here, (x^*, y^*, z^*) represents the Cartesian coordinates of the active-site in the 3-dimensional structural model of the receptor tyrosine kinase. This procedure is repeated for all tyrosine residues on the C-terminal tails of both the head and the tail monomer RTK of the asymmetric RTK dimer.

Branched Signaling Model (Fig S1, 7). Signaling through the EGF receptor is modeled with two parallel phosphorylation pathways, corresponding to tyrosine 1068 (Y1068) and tyrosine 1173 (Y1173), which have different kinetic behavior (Table 1 in main text) and different phosphorylated substrates. Phosphorylated Y1068 (Y1068p) binds only to PI3K and Grb2; Phosphorylated Y1173 (Y1173p) binds only to PLC γ and Shc. The remainder of the downstream phosphorylation cascade is left intact, as described by Schoeberl [46] and Brown [47] (Fig. S1).

Downstream Reactions. Downstream signaling reactions are interfaced with the molecular model described above. Early signaling events (reactions $\nu101$ through $\nu121$; Table S1) are implemented exactly as described by Kholodenko [8]. Later signaling events (reactions $\nu18$ through $\nu59$) are modeled exactly as described by Schoeberl [46]. These two models are interfaced by implementing a single reactive component for every species that the models shared in common (e.g., *Shc*, *Grb2*). Akt and PI3K activation are modeled exactly as described by Brown [47]. There are no species shared in common between Brown's model and the previous two.

Differences Between Mutant and Wild-type Systems. To summarize, the wild-type and mutant systems models are identical with the exception of the parameters listed in Table 1 of the main text and the following reactions which are present in the mutant (L834R).



Equations 7 and 8 represent the monomeric L834R receptor binding ATP and inhibitor, respectively. Equations 9 and 10 represent different phosphorylation sites on the receptor cytoplasmic tail entering into proximity for phosphorylation. Equations 11 and 12 are irreversible phosphorylation reactions for tyrosine 1068 and 1173, respectively. Note that for each reaction listed above, there is a corresponding reaction involving the activated form of the monomeric substrate (denoted $EGFRa$ in the model specification), which is bound to ligand. These reactions are kinetically identical to the ones listed above. The complete model specification for the mutant system is listed in Table S1. For brevity, the model for the wild-type system is not shown. It can be easily constructed by removing the mutant-specific reactions and restoring the wild-type phosphorylation parameters.

Parameter Optimization by Genetic Algorithm

Published and calculated parameters are optimized by sampling each parameter (except [EGFR], [EGF], and [Inh] (inhibitor)) from a log-normal distribution (μ = default value; $\sigma^2 = 0.25$ * default value). Newly parameterized systems are scored by comparison to experimental time-course data points (sum of squares penalty). The best parameter sets are selected by a genetic algorithm routine with the following steps:

- Exchange parameters between individuals at rate $\rho = 0.15$ (scattered, not contiguous, genetic crossover)
- Mutate all parameter-sets in population at rate $\mu = 0.15$ (resample for log-normal distribution)
- Eliminate one-third of individuals with weak fitness (individuals are eliminated in proportion to their fitness rank within the population)
- Repeat for 1000 generations

The best ten parameter-sets are kept and system output is compared to experimental time-course data points. An example time course trace from a high scoring parameter set is shown in Figure S2.

Figure S1: Schematic for branched, short-term signaling model and connection to downstream signaling components. Kinetic schemes for (1) ligand binding, (2) dimerization, (3) ATP binding, (4) intramolecular diffusion, (5,6) phosphorylation, and (7) docking reactions are described in detail in the supplementary text.

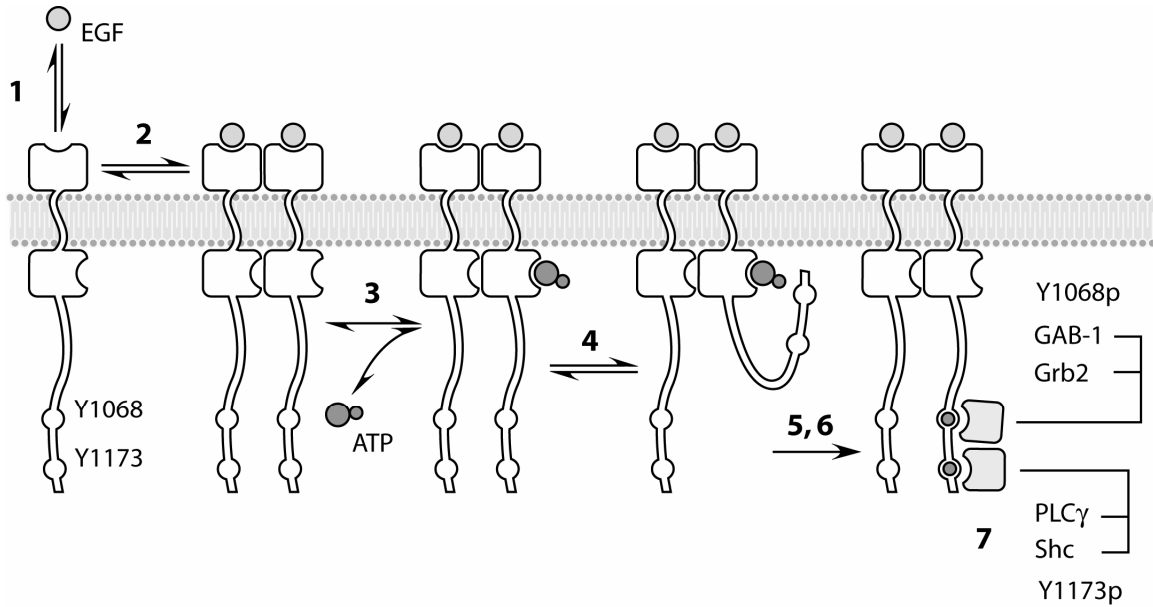


Figure S2: (a) Example time-course trace from high-scoring parameter set. (b) Experimental time-course data used to calibrate the system parameters (obtained from [48]).

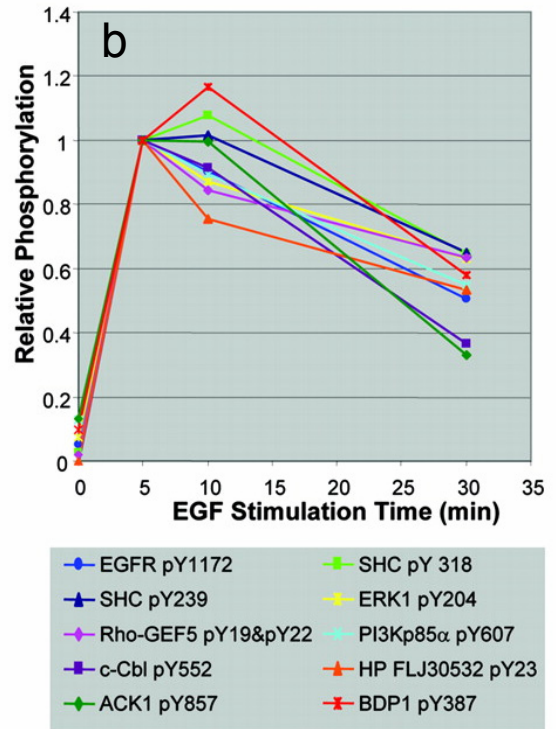
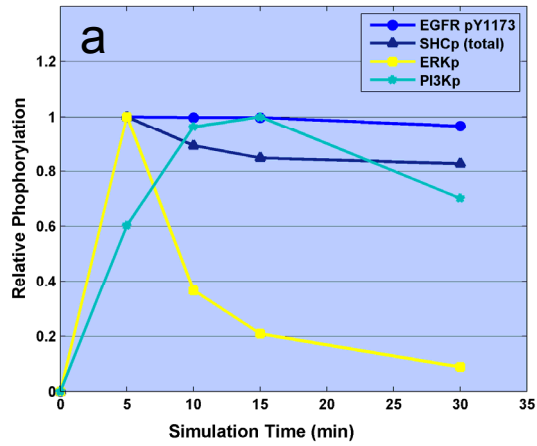


Table S1: A short-hand description (<http://www.staff.ncl.ac.uk/d.j.wilkinson/software/sbml-sh/>) of the systems models used for the wild-type and L834R deterministic models (section Methods section of main text). The models are identical except where indicated by comments. Specifically, the L834R model contains 12 species and 12 reactions that are not part of the wild-type model. Values are taken from the literature or were estimated *de novo* as described in the text and summarized in Table 2. All concentrations are in nM. An SBML compatible file of this table is also provided as supplementary material.

```

-----
@model:2.2.0="l834r_full"
@compartments
cell=1 "cell"
@species
cell:[EGF]=0.0 "EGF"
cell:[Inh]=1.0 "Inh"
cell:[EGFR]=100.0 "EGFR"
cell:[EGFRa]=0.0 "EGFRa"
cell:[Dimer0]=0.0 "Dimer0"
cell:[Dimer0_ATP]=0.0 "Dimer0_ATP"
cell:[Dimer0_Inh]=0.0 "Dimer0_Inh"
cell:[Dimer0_ATP_Y1068]=0.0 "Dimer0_ATP_Y1068"
cell:[Dimer0Y1068p]=0.0 "Dimer0Y1068p"
cell:[Dimer0Y1068p_ATP]=0.0 "Dimer0Y1068p_ATP"
cell:[Dimer0Y1068p_Inh]=0.0 "Dimer0Y1068p_Inh"
cell:[Dimer0Y1068p_ATP_Y1068]=0.0 "Dimer0Y1068p_ATP_Y1068"
cell:[Dimer0Y1068pY1068p]=0.0 "Dimer0Y1068pY1068p"
cell:[Dimer0_ATP_Y1173]=0.0 "Dimer0_ATP_Y1173"
cell:[Dimer0Y1173p]=0.0 "Dimer0Y1173p"
cell:[Dimer0Y1173p_ATP]=0.0 "Dimer0Y1173p_ATP"
cell:[Dimer0Y1173p_Inh]=0.0 "Dimer0Y1173p_Inh"
cell:[Dimer0Y1173p_ATP_Y1173]=0.0 "Dimer0Y1173p_ATP_Y1173"
cell:[Dimer0Y1173pY1173p]=0.0 "Dimer0Y1173pY1173p"
cell:[Dimer1]=0.0 "Dimer1"
cell:[Dimer1_ATP]=0.0 "Dimer1_ATP"
cell:[Dimer1_Inh]=0.0 "Dimer1_Inh"
cell:[Dimer1_ATP_Y1068]=0.0 "Dimer1_ATP_Y1068"
cell:[Dimer1Y1068p]=0.0 "Dimer1Y1068p"
cell:[Dimer1Y1068p_ATP]=0.0 "Dimer1Y1068p_ATP"
cell:[Dimer1Y1068p_Inh]=0.0 "Dimer1Y1068p_Inh"
cell:[Dimer1Y1068p_ATP_Y1068]=0.0 "Dimer1Y1068p_ATP_Y1068"
cell:[Dimer1Y1068pY1068p]=0.0 "Dimer1Y1068pY1068p"
cell:[Dimer1_ATP_Y1173]=0.0 "Dimer1_ATP_Y1173"
cell:[Dimer1Y1173p]=0.0 "Dimer1Y1173p"
cell:[Dimer1Y1173p_ATP]=0.0 "Dimer1Y1173p_ATP"
cell:[Dimer1Y1173p_Inh]=0.0 "Dimer1Y1173p_Inh"
cell:[Dimer1Y1173p_ATP_Y1173]=0.0 "Dimer1Y1173p_ATP_Y1173"
cell:[Dimer1Y1173pY1173p]=0.0 "Dimer1Y1173pY1173p"
cell:[Dimer2]=0.0 "Dimer2"
cell:[Dimer2_ATP]=0.0 "Dimer2_ATP"
cell:[Dimer2_Inh]=0.0 "Dimer2_Inh"
cell:[Dimer2_ATP_Y1068]=0.0 "Dimer2_ATP_Y1068"
cell:[Dimer2Y1068p]=0.0 "Dimer2Y1068p"
cell:[Dimer2Y1068p_ATP]=0.0 "Dimer2Y1068p_ATP"
cell:[Dimer2Y1068p_Inh]=0.0 "Dimer2Y1068p_Inh"
cell:[Dimer2Y1068p_ATP_Y1068]=0.0 "Dimer2Y1068p_ATP_Y1068"
cell:[Dimer2Y1068pY1068p]=0.0 "Dimer2Y1068pY1068p"
cell:[Dimer2_ATP_Y1173]=0.0 "Dimer2_ATP_Y1173"
cell:[Dimer2Y1173p]=0.0 "Dimer2Y1173p"
cell:[Dimer2Y1173p_ATP]=0.0 "Dimer2Y1173p_ATP"
cell:[Dimer2Y1173p_Inh]=0.0 "Dimer2Y1173p_Inh"
cell:[Dimer2Y1173p_ATP_Y1173]=0.0 "Dimer2Y1173p_ATP_Y1173"
cell:[Dimer2Y1173pY1173p]=0.0 "Dimer2Y1173pY1173p"
cell:[TotalY1068p]=0.0 "TotalY1068p"
cell:[TotalY1173p]=0.0 "TotalY1173p"
cell:[PLCg]=105.0 "PLCg"
cell:[RPLCg]=0.0 "RPLCg"
cell:[RPLCgP]=0.0 "RPLCgP"
cell:[PLCgP]=0.0 "PLCgP"
cell:[Grb]=85.0 "Grb"
cell:[RG]=0.0 "RG"
cell:[SOS]=34.0 "SOS"
cell:[RGS]=0.0 "RGS"
cell:[GS]=0.0 "GS"
cell:[Shc]=150.0 "Shc"
cell:[RSh]=0.0 "RSh"
cell:[RShP]=0.0 "RShP"
cell:[ShP]=0.0 "ShP"
cell:[RShG]=0.0 "RShG"
cell:[ShG]=0.0 "ShG"
cell:[RShGS]=0.0 "RShGS"
cell:[ShGS]=0.0 "ShGS"
cell:[PLCgl]=0.0 "PLCgl"
cell:[RasGDP]=130.0 "RasGDP"
cell:[RasGTP]=0.0 "RasGTP"
cell:[RGSRasGDP]=0.0 "RGSRasGDP"
cell:[RGSRasGTP]=0.0 "RGSRasGTP"
cell:[RShGSRasGDP]=0.0 "RShGSRasGDP"
cell:[Raf]=140.0 "Raf"
cell:[RafRasGTP]=0.0 "RafRasGTP"
cell:[RasGTPa]=0.0 "RasGTPa"
cell:[RShGSRasGTP]=0.0 "RShGSRasGTP"
cell:[Rafa]=0.0 "Rafa"
cell:[Pase1]=80.0 "Pase1"
cell:[RafaPase]=0.0 "RafaPase"
cell:[MEK]=332.0 "MEK"
cell:[MEKRafa]=0.0 "MEKRafa"
cell:[MEKP]=0.0 "MEKP"
cell:[MEKPRafa]=0.0 "MEKPRafa"
cell:[MEKPP]=0.0 "MEKPP"
cell:[MEKPPPase2]=0.0 "MEKPPPase2"
cell:[Pase2]=80.0 "Pase2"
cell:[MEKPPase2]=0.0 "MEKPPase2"
cell:[ERK]=332.0 "ERK"
cell:[ERKMEKPP]=0.0 "ERKMEKPP"
cell:[ERKP]=0.0 "ERKP"

```

```

cell:[ERKPM EKPP]=0.0 "ERKPM EKPP"
cell:[ERKPP]=0.0 "ERKPP"
cell:[Pase3]=80.0 "Pase3"
cell:[ERKPP Pase3]=0.0 "ERKPP Pase3"
cell:[ERKPPase3]=0.0 "ERKPPase3"
cell:[PI3KInactive]=66.0 "PI3KInactive"
cell:[PI3KActive]=0.0 "PI3KActive"
cell:[AktInactive]=66.0 "AktInactive"
cell:[AktActive]=0.0 "AktActive"
cell:[Gab]=0.0 "Gab"
cell:[EGFRGab]=0.0 "EGFRGab"
cell:[EGFRGabP]=0.0 "EGFRGabP"
cell:[EGFRGrbGab]=0.0 "EGFRGrbGab"

cell:[AktPase]=20.0 "AktPase"
cell:[AktActivePase]=0.0 "AktActivePase"

# L834R-specific Species

cell:[EGFR_ATP]=0.0 "EGFR_ATP"
cell:[EGFR_Inh]=0.0 "EGFR_Inh"

cell:[EGFR_ATP_Y1068]=0.0 "EGFR_ATP_Y1068"
cell:[EGFRY1068p]=0.0 "EGFRY1068p"

cell:[EGFR_ATP_Y1173]=0.0 "EGFR_ATP_Y1173"
cell:[EGFRY1173p]=0.0 "EGFRY1173p"

cell:[EGFRa_ATP]=0.0 "EGFRa_ATP"
cell:[EGFRa_Inh]=0.0 "EGFRa_Inh"

cell:[EGFRa_ATP_Y1068]=0.0 "EGFRa_ATP_Y1068"
cell:[EGFRaY1068p]=0.0 "EGFRaY1068p"

cell:[EGFRa_ATP_Y1173]=0.0 "EGFRa_ATP_Y1173"
cell:[EGFRaY1173p]=0.0 "EGFRaY1173p"

@parameters
K_ATP=10900.0 "K_ATP"
K_Inh=6.25 "K_Inh"
onY1068=650800.0 "onY1068"
offY1068=38.5 "offY1068"
onY1173=198400.0 "onY1173"
offY1173=192.4 "offY1173"
k_onLigand = 0.003 "k_onLigand"
k_offLigand = 0.06 "k_offLigand"
k_onDimer=0.01 "k_onDimer"
k_offDimer0 = 1000.0 "k_offDimer0"
k_offDimer1 = 1000.0 "k_offDimer1"
k_offDimer2 = 0.1 "k_offDimer2"
ATP=1000000.0 "ATP"
kcat_Y1068=0.14 "kcat_Y1068"
kcat_Y1173=0.010 "kcat_Y1173"
Vmax_Dephos=450 "Vmax_Dephos"
Km_Dephos=50 "Km_Dephos"

v101_kf=0.06 "v101_kf"
v101_kb=0.2 "v101_kb"
v102_kf=1.0 "v102_kf"
v102_kb=0.05 "v102_kb"
v103_kf=0.3 "v103_kf"
v103_kb=0.006 "v103_kb"
v104_Vmax=1.0 "v104_Vmax"
v104_Km=100.0 "v104_Km"
v105_kf=0.003 "v105_kf"
v105_kb=0.05 "v105_kb"
v106_kf=0.01 "v106_kf"
v106_kb=0.06 "v106_kb"
v107_kf=0.03 "v107_kf"
v107_kb=0.0045 "v107_kb"
v108_kf=0.0015 "v108_kf"
v108_kb=0.0001 "v108_kb"
v109_kf=0.09 "v109_kf"
v109_kb=0.6 "v109_kb"
v110_kf=6.0 "v110_kf"
v110_kb=0.06 "v110_kb"
v111_kf=0.3 "v111_kf"
v111_kb=0.0009 "v111_kb"
v112_Vmax=1.7 "v112_Vmax"
v112_Km=340.0 "v112_Km"
v113_kf=0.003 "v113_kf"
v113_kb=0.1 "v113_kb"
v114_kf=0.3 "v114_kf"
v114_kb=0.0009 "v114_kb"
v115_kf=0.01 "v115_kf"
v115_kb=0.0214 "v115_kb"
v116_kf=0.12 "v116_kf"
v116_kb=0.00024 "v116_kb"
v117_kf=0.003 "v117_kf"
v117_kb=0.1 "v117_kb"
v118_kf=0.03 "v118_kf"
v118_kb=0.064 "v118_kb"
v119_kf=0.1 "v119_kf"
v119_kb=0.021 "v119_kb"
v120_kf=0.009 "v120_kf"
v120_kb=0.0429 "v120_kb"
v121_kf=1.0 "v121_kf"
v121_kb=0.03 "v121_kb"
v18_k18f=0.015 "v18_k18f"
v18_k18b=1.3 "v18_k18b"
v19_k19f=0.5 "v19_k19f"
v19_k19b=0.0001 "v19_k19b"
v20_k20f=0.0021 "v20_k20f"
v20_k20b=0.4 "v20_k20b"
v21_k21f=0.023 "v21_k21f"
v21_k21b=0.00022 "v21_k21b"
v26_k26f=0.015 "v26_k26f"
v26_k26b=1.3 "v26_k26b"
v27_k27f=0.5 "v27_k27f"
v27_k27b=0.0001 "v27_k27b"
v28_k28f=0.001 "v28_k28f"
v28_k28b=0.0053 "v28_k28b"
v29_k29f=1.0 "v29_k29f"
v29_k29b=0.0007 "v29_k29b"
v30_k30f=0.0021 "v30_k30f"
v30_k30b=0.4 "v30_k30b"
v31_k31f=0.023 "v31_k31f"
v31_k31b=0.00022 "v31_k31b"
v42_k42f=0.0717 "v42_k42f"
v42_k42b=0.2 "v42_k42b"
v43_k43f=1.0 "v43_k43f"
v43_k43b=0.0 "v43_k43b"
v44_k44f=0.0123 "v44_k44f"
v44_k44b=0.033 "v44_k44b"
v45_k45f=3.5 "v45_k45f"
v45_k45b=0.0 "v45_k45b"
v46_k46f=0.0123 "v46_k46f"
v46_k46b=0.033 "v46_k46b"
v47_k47f=2.9 "v47_k47f"
v47_k47b=0.0 "v47_k47b"
v48_k48f=0.0143 "v48_k48f"
v48_k48b=0.8 "v48_k48b"
v49_k49f=0.058 "v49_k49f"
v49_k49b=0.0 "v49_k49b"
v50_k50f=0.00027 "v50_k50f"
v50_k50b=0.5 "v50_k50b"
v51_k51f=0.058 "v51_k51f"
v51_k51b=0.0 "v51_k51b"
v52_k52f=0.0534 "v52_k52f"

```

v52_k52b=0.01833 "v52_k52b"
v53_k53f=16.0 "v53_k53f"
v53_k53b=0.0 "v53_k53b"
v54_k54f=0.0534 "v54_k54f"
v54_k54b=0.01833 "v54_k54b"
v55_k55f=5.7 "v55_k55f"
v55_k55b=0.0 "v55_k55b"
v56_k56f=0.0141 "v56_k56f"
v56_k56b=0.6 "v56_k56b"
v57_k57f=0.246 "v57_k57f"
v57_k57b=0.0 "v57_k57b"
v58_k58f=0.005 "v58_k58f"
v58_k58b=0.5 "v58_k58b"
v59_k59f=0.246 "v59_k59f"
v59_k59b=0.0 "v59_k59b"
v60_VPI3K=10.6737 "v60_VPI3K"
v60_KmPI3K=307.06 "v60_KmPI3K"
v61_VPI3KRas=0.0771067 "v61_VPI3KRas"
v61_KmPI3KRas=452.0 "v61_KmPI3KRas"
v62_kAkt=0.0566279 "v62_kAkt"
v62_KmAkt=1086.0 "v62_KmAkt"
v63_kdRaf1ByAkt=15.1212 "v63_kdRaf1ByAkt"
v63_KmRaf1ByAkt=198.0 "v63_KmRaf1ByAkt"
v64_Vmax=0.687 "v64_Vmax"
v64_Km=176000.0 "v64_Km"
v65_kf=1.0 "v65_kf"
v65_kb=0.05 "v65_kb"
v66_Vmax=1e-009 "v66_Vmax"
v66_Km=100.0 "v66_Km"
v67_kf=0.0 "v67_kf"
v67_kb=0.0 "v67_kb"
v68_k68f=0.001 "v68_k68f"
v68_k68b=0.5 "v68_k68b"
v69_k69f=0.246 "v69_k69f"
v69_k69b=0.0 "v69_k69b"

@rules

@reactions

Ligand Binding

@rr = LigandBinding "LigandBinding"
EGF + EGFR -> EGFRa
(k_onLigand * EGF * EGFR - k_offLigand * EGFRa) * cell

Dimerization

@rr=Dimerization0 "Dimerization0"
2 EGFR -> Dimer0
(k_onDimer * EGFR * EGFR - k_offDimer0 * Dimer0) * cell

@rr=Dimerization1 "Dimerization1"
EGFR + EGFRa -> Dimer1
(k_onDimer * EGFR * EGFRa - k_offDimer1 * Dimer1) * cell

@rr=Dimerization2 "Dimerization2"
EGFRa + EGFRa -> Dimer2
(k_onDimer * EGFRa * EGFRa - k_offDimer2 * Dimer2) * cell

Dimer Binding ATP

@rr=Dimer0BindingATP "Dimer0BindingATP"
Dimer0 -> Dimer0_ATP
Dimer0 * ATP / ((K_ATP*(1+(Inh/K_Inh))) + ATP)

@rr=Dimer0Y1068pBindingATP
"Dimer0Y1068pBindingATP"

Dimer0Y1068p -> Dimer0Y1068p_ATP
Dimer0Y1068p * ATP / ((K_ATP*(1+(Inh/K_Inh))) + ATP)

@rr=Dimer0Y1173pBindingATP
"Dimer0Y1173pBindingATP"
Dimer0Y1173p -> Dimer0Y1173p_ATP
Dimer0Y1173p * ATP / ((K_ATP*(1+(Inh/K_Inh))) + ATP)

@rr=Dimer1BindingATP "Dimer1BindingATP"
Dimer1 -> Dimer1_ATP
Dimer1 * ATP / ((K_ATP*(1+(Inh/K_Inh))) + ATP)

@rr=Dimer1Y1068pBindingATP
"Dimer1Y1068pBindingATP"
Dimer1Y1068p -> Dimer1Y1068p_ATP
Dimer1Y1068p * ATP / ((K_ATP*(1+(Inh/K_Inh))) + ATP)

@rr=Dimer1Y1173pBindingATP
"Dimer1Y1173pBindingATP"
Dimer1Y1173p -> Dimer1Y1173p_ATP
Dimer1Y1173p * ATP / ((K_ATP*(1+(Inh/K_Inh))) + ATP)

@rr=Dimer2BindingATP "Dimer2BindingATP"
Dimer2 -> Dimer2_ATP
Dimer2 * ATP / ((K_ATP*(1+(Inh/K_Inh))) + ATP)

@rr=Dimer2Y1068pBindingATP
"Dimer2Y1068pBindingATP"
Dimer2Y1068p -> Dimer2Y1068p_ATP
Dimer2Y1068p * ATP / ((K_ATP*(1+(Inh/K_Inh))) + ATP)

@rr=Dimer2Y1173pBindingATP
"Dimer2Y1173pBindingATP"
Dimer2Y1173p -> Dimer2Y1173p_ATP
Dimer2Y1173p * ATP / ((K_ATP*(1+(Inh/K_Inh))) + ATP)

Monomer Binding ATP (L834R-specific)

@rr=EGFRBindingATP "EGFRBindingATP"
EGFR -> EGFR_ATP
EGFR * ATP / ((K_ATP*(1+(Inh/K_Inh))) + ATP)

@rr=EGFRaBindingATP "EGFRaBindingATP"
EGFRa -> EGFRa_ATP
EGFRa * ATP / ((K_ATP*(1+(Inh/K_Inh))) + ATP)

Dimer Binding Inhibitor

@rr=Dimer0BindingInh "Dimer0BindingInh"
Dimer0 + Inh -> Dimer0_Inh
Dimer0 * Inh / ((K_Inh*(1+(ATP/K_ATP))) + Inh)

@rr=Dimer0Y1068pBindingInh "Dimer0Y1068pBindingInh"
Dimer0Y1068p + Inh -> Dimer0Y1068p_Inh
Dimer0Y1068p * Inh / ((K_Inh*(1+(ATP/K_ATP))) + Inh)

@rr=Dimer0Y1173pBindingInh "Dimer0Y1173pBindingInh"
Dimer0Y1173p + Inh -> Dimer0Y1173p_Inh
Dimer0Y1173p * Inh / ((K_Inh*(1+(ATP/K_ATP))) + Inh)

@rr=Dimer1BindingInh "Dimer1BindingInh"
Dimer1 + Inh -> Dimer1_Inh
Dimer1 * Inh / ((K_Inh*(1+(ATP/K_ATP))) + Inh)

@rr=Dimer1Y1068pBindingInh "Dimer1Y1068pBindingInh"
Dimer1Y1068p + Inh -> Dimer1Y1068p_Inh
Dimer1Y1068p * Inh / ((K_Inh*(1+(ATP/K_ATP))) + Inh)

@rr=Dimer1Y1173pBindingInh "Dimer1Y1173pBindingInh"
Dimer1Y1173p + Inh -> Dimer1Y1173p_Inh

Dimer1Y1173p * Inh / ((K_Inh*(1+(ATP/K_ATP))) + Inh)

@rr=Dimer2BindingInh "Dimer2BindingInh"
Dimer2 + Inh -> Dimer2_Inh
Dimer2 * Inh / ((K_Inh*(1+(ATP/K_ATP))) + Inh)

@rr=Dimer2Y1068pBindingInh "Dimer2Y1068pBindingInh"
Dimer2Y1068p + Inh -> Dimer2Y1068p_Inh
Dimer2Y1068p * Inh / ((K_Inh*(1+(ATP/K_ATP))) + Inh)

@rr=Dimer2Y1173pBindingInh "Dimer2Y1173pBindingInh"
Dimer2Y1173p + Inh -> Dimer2Y1173p_Inh
Dimer2Y1173p * Inh / ((K_Inh*(1+(ATP/K_ATP))) + Inh)

Monomer Binding Inh (L834R-specific)

@rr=EGFRBindingInh "EGFRBindingInh"
EGFR + Inh -> EGFR_Inh
EGFR * Inh / ((K_Inh*(1+(ATP/K_ATP))) + Inh)

@rr=EGFRaBindingInh "EGFRaBindingInh"
EGFRa + Inh -> EGFRa_Inh
EGFRa * Inh / ((K_Inh*(1+(ATP/K_ATP))) + Inh)

Peptide Entering Proximity

@rr=Y1068nearsDimer0_ATP "Y1068nearsDimer0_ATP"
Dimer0_ATP -> Dimer0_ATP_Y1068
(onY1068 * Dimer0_ATP - offY1068 * Dimer0_ATP_Y1068)

@rr=Y1068nearsDimer0Y1068p_ATP
"Y1068nearsDimer0Y1068p_ATP"
Dimer0Y1068p_ATP -> Dimer0Y1068p_ATP_Y1068
(onY1068 * Dimer0Y1068p_ATP - offY1068 *
Dimer0Y1068p_ATP_Y1068)

@rr=Y1068nearsDimer1_ATP "Y1068nearsDimer1_ATP"
Dimer1_ATP -> Dimer1_ATP_Y1068
(onY1068 * Dimer1_ATP - offY1068 * Dimer1_ATP_Y1068)

@rr=Y1068nearsDimer1Y1068p_ATP
"Y1068nearsDimer1Y1068p_ATP"
Dimer1Y1068p_ATP -> Dimer1Y1068p_ATP_Y1068
(onY1068 * Dimer1Y1068p_ATP - offY1068 *
Dimer1Y1068p_ATP_Y1068)

@rr=Y1068nearsDimer2_ATP "Y1068nearsDimer2_ATP"
Dimer2_ATP -> Dimer2_ATP_Y1068
(onY1068 * Dimer2_ATP - offY1068 * Dimer2_ATP_Y1068)

@rr=Y1068nearsDimer2Y1068p_ATP
"Y1068nearsDimer2Y1068p_ATP"
Dimer2Y1068p_ATP -> Dimer2Y1068p_ATP_Y1068
(onY1068 * Dimer2Y1068p_ATP - offY1068 *
Dimer2Y1068p_ATP_Y1068)

@rr=Y1173nearsDimer0_ATP "Y1173nearsDimer0_ATP"
Dimer0_ATP -> Dimer0_ATP_Y1173
(onY1173 * Dimer0_ATP - offY1173 * Dimer0_ATP_Y1173)

@rr=Y1173nearsDimer0Y1173p_ATP
"Y1173nearsDimer0Y1173p_ATP"
Dimer0Y1173p_ATP -> Dimer0Y1173p_ATP_Y1173
(onY1173 * Dimer0Y1173p_ATP - offY1173 *
Dimer0Y1173p_ATP_Y1173)

@rr=Y1173nearsDimer1_ATP "Y1173nearsDimer1_ATP"
Dimer1_ATP -> Dimer1_ATP_Y1173
(onY1173 * Dimer1_ATP - offY1173 * Dimer1_ATP_Y1173)

@rr=Y1173nearsDimer1Y1173p_ATP
"Y1173nearsDimer1Y1173p_ATP"
Dimer1Y1173p_ATP -> Dimer1Y1173p_ATP_Y1173
(onY1173 * Dimer1Y1173p_ATP - offY1173 *
Dimer1Y1173p_ATP_Y1173)

@rr=Y1173nearsDimer2_ATP "Y1173nearsDimer2_ATP"
Dimer2_ATP -> Dimer2_ATP_Y1173
(onY1173 * Dimer2_ATP - offY1173 * Dimer2_ATP_Y1173)

@rr=Y1173nearsDimer2Y1173p_ATP
"Y1173nearsDimer2Y1173p_ATP"
Dimer2Y1173p_ATP -> Dimer2Y1173p_ATP_Y1173
(onY1173 * Dimer2Y1173p_ATP - offY1173 *
Dimer2Y1173p_ATP_Y1173)

Peptide Entering Monomer Proximity (L834R-specific)

@rr=Y1068nearsEGFR_ATP "Y1068nearsEGFR_ATP"
EGFR_ATP -> EGFR_ATP_Y1068
(onY1068 * EGFR_ATP - offY1068 * EGFR_ATP_Y1068)

@rr=Y1068nearsEGFRa_ATP "Y1068nearsEGFRa_ATP"
EGFRa_ATP -> EGFRa_ATP_Y1068
(onY1068 * EGFRa_ATP - offY1068 * EGFRa_ATP_Y1068)

@rr=Y1173nearsEGFR_ATP "Y1173nearsEGFR_ATP"
EGFR_ATP -> EGFR_ATP_Y1173
(onY1173 * EGFR_ATP - offY1173 * EGFR_ATP_Y1173)

@rr=Y1173nearsEGFRa_ATP "Y1173nearsEGFRa_ATP"
EGFRa_ATP -> EGFRa_ATP_Y1173
(onY1173 * EGFRa_ATP - offY1173 * EGFRa_ATP_Y1173)

Catalysis of Phosphorylation (Irreversible)

@r=PhosphorylationOfDimer0_ATP_Y1068
"PhosphorylationOfDimer0_ATP_Y1068"
Dimer0_ATP_Y1068 -> Dimer0Y1068p + TotalY1068p
kcat_Y1068 * Dimer0_ATP_Y1068

@r=PhosphorylationOfDimer0Y1068p_ATP_Y1068
"PhosphorylationOfDimer0Y1068p_ATP_Y1068"
Dimer0Y1068p_ATP_Y1068 -> Dimer0Y1068pY1068p +
TotalY1068p
kcat_Y1068 * Dimer0Y1068p_ATP_Y1068

@r=PhosphorylationOfDimer1_ATP_Y1068
"PhosphorylationOfDimer1_ATP_Y1068"
Dimer1_ATP_Y1068 -> Dimer1Y1068p + TotalY1068p
kcat_Y1068 * Dimer1_ATP_Y1068

@r=PhosphorylationOfDimer1Y1068p_ATP_Y1068
"PhosphorylationOfDimer1Y1068p_ATP_Y1068"
Dimer1Y1068p_ATP_Y1068 -> Dimer1Y1068pY1068p +
TotalY1068p
kcat_Y1068 * Dimer1Y1068p_ATP_Y1068

@r=PhosphorylationOfDimer2_ATP_Y1068
"PhosphorylationOfDimer2_ATP_Y1068"
Dimer2_ATP_Y1068 -> Dimer2Y1068p + TotalY1068p
kcat_Y1068 * Dimer2_ATP_Y1068

@r=PhosphorylationOfDimer2Y1068p_ATP_Y1068
"PhosphorylationOfDimer2Y1068p_ATP_Y1068"
Dimer2Y1068p_ATP_Y1068 -> Dimer2Y1068pY1068p +
TotalY1068p
kcat_Y1068 * Dimer2Y1068p_ATP_Y1068

@r=PhosphorylationOfDimer0_ATP_Y1173
 "PhosphorylationOfDimer0_ATP_Y1173"
 Dimer0_ATP_Y1173 -> Dimer0Y1173p + TotalY1173p
 kcat_Y1173 * Dimer0_ATP_Y1173

@r=PhosphorylationOfDimer0Y1173p_ATP_Y1173
 "PhosphorylationOfDimer0Y1173p_ATP_Y1173"
 Dimer0Y1173p_ATP_Y1173 -> Dimer0Y1173pY1173p + TotalY1173p
 kcat_Y1173 * Dimer0Y1173p_ATP_Y1173

@r=PhosphorylationOfDimer1_ATP_Y1173
 "PhosphorylationOfDimer1_ATP_Y1173"
 Dimer1_ATP_Y1173 -> Dimer1Y1173p + TotalY1173p
 kcat_Y1173 * Dimer1_ATP_Y1173

@r=PhosphorylationOfDimer1Y1173p_ATP_Y1173
 "PhosphorylationOfDimer1Y1173p_ATP_Y1173"
 Dimer1Y1173p_ATP_Y1173 -> Dimer1Y1173pY1173p + TotalY1173p
 kcat_Y1173 * Dimer1Y1173p_ATP_Y1173

@r=PhosphorylationOfDimer2_ATP_Y1173
 "PhosphorylationOfDimer2_ATP_Y1173"
 Dimer2_ATP_Y1173 -> Dimer2Y1173p + TotalY1173p
 kcat_Y1173 * Dimer2_ATP_Y1173

@r=PhosphorylationOfDimer2Y1173p_ATP_Y1173
 "PhosphorylationOfDimer2Y1173p_ATP_Y1173"
 Dimer2Y1173p_ATP_Y1173 -> Dimer2Y1173pY1173p + TotalY1173p
 kcat_Y1173 * Dimer2Y1173p_ATP_Y1173

Catalysis of Monomer Phosphorylation (L834R-specific)

@r=PhosphorylationOfEGFR_ATP_Y1068
 "PhosphorylationOfEGFR_ATP_Y1068"
 EGFR_ATP_Y1068 -> EGFRY1068p + TotalY1068p
 kcat_Y1068 * EGFR_ATP_Y1068

@r=PhosphorylationOfEGFRa_ATP_Y1068
 "PhosphorylationOfEGFRa_ATP_Y1068"
 EGFRa_ATP_Y1068 -> EGFRaY1068p + TotalY1068p
 kcat_Y1068 * EGFRa_ATP_Y1068

@r=PhosphorylationOfEGFR_ATP_Y1173
 "PhosphorylationOfEGFR_ATP_Y1173"
 EGFR_ATP_Y1173 -> EGFRY1173p + TotalY1173p
 kcat_Y1173 * EGFR_ATP_Y1173

@r=PhosphorylationOfEGFRa_ATP_Y1173
 "PhosphorylationOfEGFRa_ATP_Y1173"
 EGFRa_ATP_Y1173 -> EGFRaY1173p + TotalY1173p
 kcat_Y1173 * EGFRa_ATP_Y1173

Receptor Dephosphorylation

@rr=DephosphorylationOfY1068p
 "DephosphorylationOfY1068p"
 TotalY1068p -> EGFR
 Vmax_Dephos * TotalY1068p / (Km_Dephos + TotalY1068p)

@rr=DephosphorylationOfY1173p
 "DephosphorylationOfY1173p"
 TotalY1173p -> EGFR
 Vmax_Dephos * TotalY1173p / (Km_Dephos + TotalY1173p)

@rr=v101 "v101"
 TotalY1173p+PLCg -> RPLCg
 (v101_kf * TotalY1173p * PLCg - v101_kb * RPLCg) * cell

@rr=v102 "v102"
 RPLCg -> RPLCgP
 (v102_kf * RPLCg - v102_kb * RPLCgP) * cell

@rr=v103 "v103"
 RPLCgP -> TotalY1173p+PLCgP
 (v103_kf * RPLCgP - v103_kb * TotalY1173p * PLCgP) * cell

@rr=v104 "v104"
 PLCgP -> PLCg
 v104_Vmax * PLCgP / (v104_Km + PLCgP) * cell

@rr=v105 "v105"
 TotalY1068p+Grb -> RG
 (v105_kf * TotalY1068p * Grb - v105_kb * RG) * cell

@rr=v106 "v106"
 RG+SOS -> RGS
 (v106_kf * RG * SOS - v106_kb * RGS) * cell

@rr=v107 "v107"
 RGS -> TotalY1068p+GS
 (v107_kf * RGS - v107_kb * TotalY1068p * GS) * cell

@rr=v108 "v108"
 GS -> Grb+SOS
 (v108_kf * GS - v108_kb * Grb * SOS) * cell

@rr=v109 "v109"
 TotalY1173p+Shc -> RSh
 (v109_kf * TotalY1173p * Shc - v109_kb * RSh) * cell

@rr=v110 "v110"
 RSh -> RShP
 (v110_kf * RSh - v110_kb * RShP) * cell

@rr=v111 "v111"
 RShP -> TotalY1173p+ShP
 (v111_kf * RShP - v111_kb * ShP * TotalY1173p) * cell

@rr=v112 "v112"
 ShP -> Shc
 v112_Vmax * ShP / (v112_Km + ShP) * cell

@rr=v113 "v113"
 Grb+RShP -> RShG
 (v113_kf * RShP * Grb - v113_kb * RShG) * cell

@rr=v114 "v114"
 RShG -> TotalY1173p+ShG
 (v114_kf * RShG - v114_kb * TotalY1173p * ShG) * cell

@rr=v115 "v115"
 SOS+RShG -> RShGS
 (v115_kf * RShG * SOS - v115_kb * RShGS) * cell

@rr=v116 "v116"
 RShGS -> TotalY1173p+ShGS
 (v116_kf * RShGS - v116_kb * ShGS * TotalY1173p) * cell

@rr=v117 "v117"
 Grb+ShP -> ShG
 (v117_kf * ShP * Grb - v117_kb * ShG) * cell

@rr=v118 "v118"
 SOS+ShG -> ShGS
 (v118_kf * ShG * SOS - v118_kb * ShGS) * cell

@rr=v119 "v119"
 ShGS -> GS+ShP
 (v119_kf * ShGS - v119_kb * ShP * GS) * cell

@rr=v120 "v120"
 GS+RShP -> RShGS
 (v120_kf * RShP * GS - v120_kb * RShGS) * cell

@rr=v121 "v121"
 PLCgP -> PLCgl
 v121_kf * PLCgP * cell

@rr=v18 "v18"
 RGS+RasGDP -> RGSRasGDP
 (v18_k18f * RasGDP * RGS - v18_k18b * RGSRasGDP) * cell

@rr=v19 "v19"
 RGSRasGDP -> RGS+RasGTP
 (v19_k19f * RGSRasGDP - v19_k19b * RGS * RasGTP) * cell

@rr=v20 "v20"

RGS+RasGTPa -> RGS+RasGTP
 (v20_k20f * RasGTPa * RGS - v20_k20b * RGS+RasGTP) * cell
 @rr=v21 "v21"
 RGS+RasGTP -> RGS+RasGDP
 (v21_k21f * RGS+RasGTP - v21_k21b * RGS * RasGDP) * cell
 @rr=v26 "v26"
 RShGS+RasGDP -> RShGS+RasGDP
 (v26_k26f * RasGDP * RShGS - v26_k26b * RShGS+RasGDP) * cell
 @rr=v27 "v27"
 RShGS+RasGDP -> RShGS+RasGTP
 (v27_k27f * RShGS+RasGDP - v27_k27b * RShGS * RasGTP) * cell
 @rr=v28 "v28"
 RasGTP+Raf -> Raf+RasGTP
 (v28_k28f * RasGTP * Raf - v28_k28b * Raf+RasGTP) * cell
 @rr=v29 "v29"
 Raf+RasGTP -> Raf+RasGTPa
 (v29_k29f * Raf+RasGTP - v29_k29b * Raf+RasGTPa * Raf) * cell
 @rr=v30 "v30"
 RShGS+RasGTPa -> RShGS+RasGTP
 (v30_k30f * RShGS * RasGTPa - v30_k30b * RShGS+RasGTP) * cell
 @rr=v31 "v31"
 RShGS+RasGTP -> RShGS+RasGDP
 (v31_k31f * RShGS+RasGTP - v31_k31b * RShGS * RasGDP) * cell
 @rr=v42 "v42"
 Raf+Pase1 -> Raf+Pase
 (v42_k42f * Pase1 * Raf - v42_k42b * Raf+Pase) * cell
 @rr=v43 "v43"
 Raf+Pase -> Raf+Pase1
 (v43_k43f * Raf+Pase - v43_k43b * Raf * Pase1) * cell
 @rr=v44 "v44"
 Raf+MEK -> MEK+Raf
 (v44_k44f * MEK * Raf - v44_k44b * MEK+Raf) * cell
 @rr=v45 "v45"
 MEK+Raf -> MEK+Raf
 (v45_k45f * MEK+Raf - v45_k45b * MEK * Raf) * cell
 @rr=v46 "v46"
 Raf+MEK -> MEK+Raf
 (v46_k46f * MEK * Raf - v46_k46b * MEK+Raf) * cell
 @rr=v47 "v47"
 MEK+Raf -> MEK+Raf
 (v47_k47f * MEK+Raf - v47_k47b * MEK * Raf) * cell
 @rr=v48 "v48"
 MEK+Pase2 -> MEK+Pase2
 (v48_k48f * MEK * Pase2 - v48_k48b * MEK+Pase2) * cell
 @rr=v49 "v49"
 MEK+Pase2 -> MEK+Pase2
 (v49_k49f * MEK+Pase2 - v49_k49b * MEK * Pase2) * cell
 @rr=v50 "v50"
 MEK+Pase2 -> MEK+Pase2
 (v50_k50f * MEK * Pase2 - v50_k50b * MEK+Pase2) * cell
 @rr=v51 "v51"
 MEK+Pase2 -> MEK+Pase2
 (v51_k51f * MEK+Pase2 - v51_k51b * MEK * Pase2) * cell
 @rr=v52 "v52"
 MEK+ERK -> ERK+MEK

(v52_k52f * ERK * MEK - v52_k52b * ERK+MEK) * cell
 @rr=v53 "v53"
 ERK+MEK -> ERK+MEK
 (v53_k53f * ERK+MEK - v53_k53b * ERK * MEK) * cell
 @rr=v54 "v54"
 MEK+ERK -> ERK+MEK
 (v54_k54f * MEK * ERK - v54_k54b * ERK+MEK) * cell
 @rr=v55 "v55"
 ERK+MEK -> ERK+MEK
 (v55_k55f * ERK+MEK - v55_k55b * ERK * MEK) * cell
 @rr=v56 "v56"
 ERK+Pase3 -> ERK+Pase3
 (v56_k56f * ERK * Pase3 - v56_k56b * ERK+Pase3) * cell
 @rr=v57 "v57"
 ERK+Pase3 -> ERK+Pase3
 (v57_k57f * ERK+Pase3 - v57_k57b * ERK * Pase3) * cell
 @rr=v58 "v58"
 ERK+Pase3 -> ERK+Pase3
 (v58_k58f * Pase3 * ERK - v58_k58b * ERK+Pase3) * cell
 @rr=v59 "v59"
 ERK+Pase3 -> ERK+Pase3
 (v59_k59f * ERK+Pase3 - v59_k59b * ERK * Pase3) * cell
 @rr=v60 "v60"
 PI3KInactive -> PI3KActive : TotalY1068p
 v60_VPI3K * TotalY1068p * PI3KInactive / (PI3KInactive + v60_KmPI3K) * cell
 @rr=v61 "v61"
 PI3KInactive -> PI3KActive : RasGTPa
 v61_VPI3KRas * RasGTPa * PI3KInactive / (PI3KInactive + v61_KmPI3KRas) * cell
 @rr=v62 "v62"
 AktInactive -> AktActive : PI3KActive
 v62_kAkt * PI3KActive * AktInactive / (AktInactive + v62_KmAkt) * cell
 @rr=v63 "v63"
 Raf -> Raf : AktActive
 v63_kdRafByAkt * AktActive * Raf / (Raf + v63_KmRafByAkt) * cell
 @rr=v64 "v64"
 TotalY1068p+Gab -> EGFRGab
 v64_Vmax * TotalY1068p * Gab / (EGFRGab + v64_Km) * cell
 @rr=v65 "v65"
 EGFRGab -> EGFRGab
 (v65_kf * EGFRGab - v65_kb * EGFRGab) * cell
 @rr=v66 "v66"
 EGFRGab -> EGFRGab
 v66_Vmax * EGFRGab / (v66_Km + EGFRGab) * cell
 @rr=v67 "v67"
 RG+EGFRGab -> EGFRGrbGab
 (v67_kf * RG * EGFRGab - v67_kb * EGFRGrbGab) * cell
 @rr=v68 "v68"
 AktActive + AktPase -> AktActivePase
 (v68_k68f * AktPase * AktActive - v68_k68b * AktActivePase) * cell
 @rr=v69 "v69"
 AktActivePase -> AktPase
 (v69_k69f * AktActivePase - v69_k69b * AktInactive * AktPase) * cell

References

1. Liu, Y., et al., *A Multiscale Computational Approach to Dissect Early Events in the Erb Family Receptor Mediated Activation, Differential Signaling, and Relevance to Oncogenic Transformations*. Annals of Biomedical Engineering, 2007. **35**(6): p. 1012-1025.
2. Schlessinger, J., *Common and distinct elements in cellular signaling between EGF and FGF receptors*. Science, 2004. **306**: p. 1506-1507.
3. Schlessinger, J., *Cell signaling by receptor tyrosine kinases*. Cell, 2000. **103**: p. 211-225.
4. Jorrinssen, R.N., *Epidermal growth factor receptor: mechanism of activation and signaling*. Exp. Cell. Res., 2003. **284**: p. 31-53.
5. Shawyer, L.K., D. Slamon, and a.A. Ullrich, *Smart drugs: tyrosine kinase inhibitors in cancer therapy*. Cell, 2002. **1**: p. 117-123.
6. Chatterjee, A. and et al., *Binomial distribution based tau-leap accelerated stochastic simulation*. J.Chem.Phys., 2005: p. 024112.
7. al., A.C.e., *Binomial distribution based tau-leap accelerated stochastic simulation*. J.Chem.Phys., 2005: p. 024112.
8. Kholodenko, B.N., et al., *Quantification of short term signaling by the epidermal growth factor receptor*. Journal of Biological Chemistry, 1999. **274**(42): p. 30169-30181.
9. Aksan, I. and M.L. Kurnaz, *Computer-based model for the regulation of MAPK activation*. J. Receptors Signal Transduction, 2003. **23**: p. 197-209.
10. Asthagiri, A. and D.A. Lauffenburger, *Cell signaling models in bioengineering*. Annu. Rev. Biomed. eng., 2000. **2**: p. 32-53.
11. Miller, J.H. and F. Zhang, *Large scale simulation of cellular signaling processes*. Parallel Comput., 2004.
12. Schoeberl, B., et al., *Computational modeling of the dynamics of MAPKinase cascade activated by surface and internalized receptors*. Nature Biotech., 2002. **20**: p. 370-375.
13. Uyemura, T., et al., *Single-molecule analysis of epidermal growth factor signaling that leads to ultrasensitive calcium response*. Biophys J., 2005.
14. Bhalla, U.S., P.T. Ram, and R. Iyengar, *MAPKinase phosphatase as a locus of flexibility in a mitogen activated protein kinase signaling network*. Science, 2002. **297**: p. 1018-1023.
15. Bhalla, U.S. and R. Iyengar, *Emergent properties of biological networks*. Science, 1999. **283**: p. 381-387.
16. Weng, G., U.S. Bhalla, and R. Iyengar, *Complexities in biological signaling systems*. Science, 1999. **284**: p. 92-96.
17. Haugh, J.M., A. Wells, and D.A. Lauffenburger, *Mathematical modeling of epidermal growth factor receptor signaling through the phospholipase C pathway: mechanistic insights and predictions for molecular interventions*. Biotechnol Bioeng, 2000. **70**(2): p. 225-38.
18. Canteley, L.C., *The PI3K pathway*. Science, 2002. **296**: p. 1655-1657.
19. Brown, K.S., et al., *The statistical mechanics of complex signaling networks: nerve growth factor signaling*. Phys. Biol., 2004. **1**: p. 184-195.
20. Hatakeyama, M., et al., *A computational model on the modulation of MAPK and Akt pathways in Heregulin-induced ERB signaling*. Biochem. J., 2003. **373**: p. 451-463.
21. Rodrigues, G.A., et al., *A Novel Positive Feedback Loop Mediated by the Docking Prote in Gab1 and Phosphatidylinositol 3-Kinase in Epidermal Growth Factor Receptor Signaling*. Mol. Cell Biol., 2000. **20**: p. 1448-1459.
22. Sachsenmaler, C., *Targeting protein kinases for tumor therapy*. Onkologie, 2001. **24**: p. 346-355.
23. Mendelsohn, J. and J. Baselga, *Status of EGFR antagonists in biology and treatment of cancer*. J. Clini. Onco., 2003. **21**: p. 2782-2799.
24. Pulverer, B., *Nature insight: Cancer*. nature, 2003. **411**: p. 335-395.
25. Boerner, J.L., et al., *Phosphorylation of Y845 on the Epidermal Growth Factor Receptor Mediates Binding to the Mitochondrial Protein Cytochrome c Oxidase Subunit II*. Mol. Cell Biol., 2004. **24**: p. 7059-7071.
26. Kloth, M.T., et al., *STAT5b, a Mediator of Synergism between c-Src and the Epidermal Growth Factor Receptor*. J. Biol. Chem., 2003. **278**: p. 1671-1679.

27. Biscardi, J.S., et al., *c-Src-mediated Phosphorylation of the Epidermal Growth Factor Receptor on Tyr845 and Tyr1101 Is Associated with Modulation of Receptor Function*. J. Biol. Chem., 1999. **274**(12): p. 8335-8343.
28. Wu, W., et al., *Src-dependent phosphorylation of the epidermal growth factor receptor on tyrosine 845 is required for zinc-induced Ras activation*. Journal of Biological Chemistry, 2002. **277**(27): p. 24252-24257.
29. Haugh, J.M. and D.A. Lauffenburger, *Analysis of receptor internalization as a mechanism for modulating signal transduction*. J Theor Biol, 1998. **195**(2): p. 187-218.
30. Vieira, A.V., C. Lamaze, and S.L. Schmid, *Control of EGF Receptor signaling by clathrin-mediated endocytosis*. Science, 1996. **274**: p. 2066-2089.
31. Dikic, I., *Mechanisms controlling EGF receptor endocytosis and degradation*. Biochem. Soc. Trans., 2003. **31**: p. 1178-1181.
32. Kim, J., et al., *Regulation of EGFR internalization by GPCR*. Biochemistry, 2003. **42**: p. 2887-2894.
33. Pierce, K.L., et al., *Role of endocytosis in the activation of extracellular signal-regulated kinase cascade by sequestering and nonsequestering GPCR*. Proc. Natl. Acad. Sci. USA, 2000. **97**: p. 1489-1494.
34. Luttrell, L.M., Y. Daaka, and R.J. Lefkowitz, *Regulation of tyrosine kinase cascades by GPCR*. Curr. Opin. Cell Biol., 1999. **11**: p. 177-183.
35. Bookout, A.L., et al., *Targeting G β signaling to inhibit prostate tumor formation and growth*. J. Biol. Chem., 2003. **278**: p. 37569-37573.
36. Prenzel, N., et al., *Tyrosine kinase signalling in breast cancer Epidermal growth factor receptor: convergence point for signal integration and diversification*. Breast Cancer Res., 2000. **2**: p. 184-190.
37. Cabodi, S., et al., *Integrin regulation of epidermal growth factor (EGF) receptor and of EGF-dependent responses*. Biochem. Soc. Trans., 2004. **32**: p. 438-442.
38. Fischer, O.M., et al., *EGFR signal trans activation in cancer cells*. Biochem. Soc. Trans., 2003. **31**: p. 1203-1208.
39. Saso, K., et al., *Differential inhibition of epidermal growth factor signaling pathways in rat hepatocytes by long-term ethanol treatment*. Gastroenterology, 1997. **112**(6): p. 2073-2088.
40. Brignola, P.S., et al., *Comparison of the biochemical and kinetic properties of the type I receptor tyrosine kinase intracellular domains - Demonstration of differential sensitivity to kinase inhibitors*. Journal of Biological Chemistry, 2002. **277**(2): p. 1576-1585.
41. Fan, Y.X., et al., *Ligand regulates epidermal growth factor receptor kinase specificity - Activation increases preference for GAB1 and SHC versus autophosphorylation sites*. Journal of Biological Chemistry, 2004. **279**(37): p. 38143-38150.
42. Stamos, J., M.X. Sliwkowski, and C. Eigenbrot, *Structure of the epidermal growth factor receptor kinase domain alone and in complex with a 4-anilinoquinazoline inhibitor*. J Biol Chem, 2002. **277**(48): p. 46265-72.
43. Zhang, X., et al., *An allosteric mechanism for activation of the kinase domain of epidermal growth factor receptor*. Cell, 2006. **125**(6): p. 1137-49.
44. Dill, K.A., *Molecular driving forces*. 2003, New York: Garland Science.
45. Zhou, H.X., *Loops in proteins can be modeled as worm-like chains*. Journal of Physical Chemistry B, 2001. **105**(29): p. 6763-6766.
46. Schoeberl, B., et al., *Computational modeling of the dynamics of the MAP kinase cascade activated by surface and internalized EGF receptors*. Nature Biotechnology, 2002. **20**(4): p. 370-375.
47. Brown, K.S. and J.P. Sethna, *Statistical mechanical approaches to models with many poorly known parameters*. Physical Review E, 2003. **68**(2): p. 021904.
48. Zhang, Y., et al., *Time-resolved mass spectrometry of tyrosine phosphorylation sites in the epidermal growth factor receptor signaling network reveals dynamic modules*. Molecular & Cellular Proteomics, 2005. **4**(9): p. 1240-1250.